Colloid Polym Sci (2014) 292:1701–1710
DOI 10.1007/s00396-014-3232-x

ORIGINAL CONTRIBUTION

Modeling the effect of molecular architecture of comb polymers on the behavior of Al_2O_3 dispersions using charge/composition factors (CCF)

Yoram de Hazan · Judit Wilkens-Heinecke · Thomas Graule

Received: 14 January 2014 / Revised: 14 March 2014 / Accepted: 10 April 2014 / Published online: 2 May 2014

Abstract In this work, we study the effect of periodicity and PEO side-chain length in four PMAA-PEO (sodium salt) comb polymers with known molecular architecture on Al_2O_3 colloidal dispersions in DI water. We introduce here charge composition factors (CCF) representing charge density of the comb polymers defined as (number of charged units in a repeating unit)/(molecular weight of a repeating unit). We find, for the first time to our knowledge, that the CCF can be used along with dispersant dosage to obtain explicit functions predicting the conductivity of the dispersants in solution, the zeta potential behavior during dispersant titrations, and the isoelectric point (IEP) of the dispersions. In addition, the dosage normalized by the CCF provides a basis for comparison for the dispersants to elucidate the trends found in adsorption and potentiometric titrations. Thus, the CCF can be used as a tool for the design of improved and new comb polymer molecular architectures.

Keywords Comb-polymer · Colloid · Al_2O_3 · Zeta-potential · Modeling · Isoelectric point · Molecular architecture · Adsorption

Y. de Hazan (✉)
ZHAW, Zurich University of Applied Sciences, School of Engineering, Technikumstrasse 9, 8401 Winterthur, Switzerland
e-mail: deha@zhaw.ch

Y. de Hazan
e-mail: ydehazan@gmail.com

Y. de Hazan · J. Wilkens-Heinecke · T. Graule
Empa, Swiss Federal Laboratories for Materials Science and Technology, Laboratory for High Performance Ceramics, 8600 Dübendorf, Switzerland

Introduction

Many applications in colloid science in general and ceramic shaping technology in particular rely on colloid stability using state of the art dispersants [1–4]. Comb polymers, especially comb polyelectrolytes, are receiving increased attention as super-plasticizers in the cement industry [5–16], surface modifying agents for colloids such as Si_3N_4 [17], WC-Co [18], MgO [18, 19], $BaTiO_3$ [20], Al_2O_3 [21–25], ZnO [22], TiO_2 and Fe_2O_3 [23], $CaCO_3$ [26], electrosteric dispersants in advanced ceramic shaping processes [2, 3, 23], and emerging class of steric dispersants for composite electroless Ni-P/ceramic coatings containing Al_2O_3, TiO_2, CeO_2 nanoparticles [4, 24].

The influence of comb polymer molecular architecture on the properties and processing of cements was studied extensively [7–15]. Insight into the dependence of adsorption, zeta potential, rheology, hydration, microstructure, and mechanical strength on the molecular architecture was obtained with synthesized dispersants having systematically varying frequency of charged groups on their backbone and/or side-chains of varying length [7–15].

In comparison, relatively few studies connecting the molecular architectures of comb polymers as dispersants for colloidal ceramic particles exist [17–22, 25, 26]. Of the properties which are more systematically studied are dispersant adsorption, zeta potential, and rheology, where the main variation is the length of comb polymer side-chain. Other studies often use commercial comb polymers where exact knowledge of molecular architecture is not known [3, 4, 23, 24].

Explicit relations regarding the conformation of comb polymers adsorbed on surfaces could be developed based on the side-chain length and frequency of repeated units (the parameters p, m, and n as defined in Fig. 1) [27, 28]. Such parameters could be related inexplicitly to the hydrodynamic radius and conformation of the comb polymers in solution using factors based on charge and molecular weight [20].

In particular, systematic investigations relating the molecular architecture of both side-chain length and its frequency on the backbone to the behavior of dispersions via explicit relationships can be of a great value for the understanding of dispersion phenomena and the design of advanced dispersants.

In our present work, we systematically compare four comb polymers with known molecular architectures as dispersants for colloidal Al_2O_3 particles. These PMAA-PEO comb polymers have different side-chain length and frequency. In addition, we demonstrate the usefulness of a factor derived from the molecular architecture of the comb polymer in normalizing and predicting explicitly the dispersant conductivity in solution; the initial rate of zeta potential change, the minimum zeta potential, and corresponding dispersant weight during dispersant titrations as well as the isoelectric point (IEP) of the dispersions as a function of dispersant concentration.

Experimental

Materials

The Al_2O_3 powder studied was TM-DAR, α-Al_2O_3 obtained from Taimei Chemicals Co., LTD, Japan. This powder has a mean particle size of 120 nm according to measurements of particle size distribution by LS230 (Beckman Coulter, USA) [22], a density of 3.98 g/cm^3, and a specific surface area of 12.5 m^2/g, measured by BET method with SA3100 (Beckman Coulter, USA) [22].

Four experimental dispersants obtained from BASF, Germany were investigated as electrosteric dispersants for Al_2O_3 dispersions. Figure 1 shows the statistical chemical structure of the comb polyelectrolytes. The synthesis of these dispersants is presented elsewhere [7]. All these anionic comb-shaped polyelectrolytes consist of a poly(methacrylic acid) (PMAA) sodium salt backbone which can adsorb on positively charged particles and poly(ethylene oxide) (PEO) side-chains, which can extend into the aqueous medium providing steric hindrance [6].

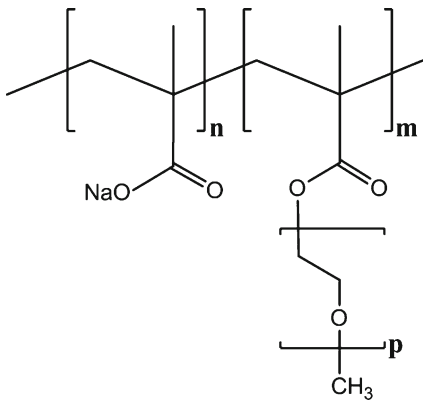

Fig. 1 Statistical chemical structure of the comb polyelectrolytes

Table 1 outlines the composition (p, n, m defined in Fig. 1) and molecular weights of the four dispersants used in this study. Dispersants B174 and B176 have relatively short side-chains consisting of 23 repeating ethylene oxide (EO) units and B178 and B179 have long side-chains consisting of 102 repeating EO units. Dispersants B174 and B178 have a relatively low frequency of charged groups in a repeating unit (two out of three groups) while dispersants B176 and B179 have a relatively high frequency of charged groups in a repeating unit (six out of seven groups).

Preparation of dispersions and dispersant solutions

Ten weight percent of TM-DAR powder were dispersed in deionized (DI) water and de-agglomerated with 0.5 mm zirconia balls (Tosho, Japan) for 4 h on a rolling mill. Particle size distribution of de-agglomerated dispersions was monitored with a laser scattering instrument, LS 230 (Beckman Coulter, USA) until the particle size distribution showed no agglomeration [22]. The electrostatically stable dispersions were separated from the zirconia balls by sieving and diluted from 10 down to 4 wt%.

The dispersant solutions in DI water were prepared at 6 wt% at pH of 4.5±0.2, adjusted with a 1 M HCl solution. This acidification procedure is performed in order to maintain similar and favorable conditions for dispersant adsorption on the particles [24].

Zeta potential and conductivity measurements in solution

ZetaProbe Analyzer (Colloidal Dynamics Inc, USA) was used for simultaneous measurement of conductivity, pH, and zeta potential. The dispersant solutions were added in a logarithmic progression series into 150 ml vessels containing 4 wt% Al_2O_3 dispersions where the measurements were carried out, with 30 s equilibrium time [24]. Following the titrations, the dispersions were ultrasonicated and remained stable during subsequent measurements [24]. Measurements of dispersant

Table 1 Characteristics of the comb polymer dispersants used in this work (n, m, and p defined in Fig. 1)

Dispersant	*p*	*n*:*m*	Mn	Mw	Mw/Mn	Characteristics
B174	23	2:1	8700	25600	2.9	Short chain/low charge
B176	23	6:1	7600	18900	2.5	Short chain/high charge
B178	102	2:1	16800	78000	4.6	Long chain/low charge
B179	102	6:1	14600	67000	4.6	Long chain/high charge

conductivity in DI water were performed in a similar fashion in the ZetaProbe Analyzer, where the dispersant solutions are added gradually to 150 ml vessel containing DI water. Potentiometric titrations were performed with 150 ml dispersion containing 4 wt% Al_2O_3 and 0–23 wt% dispersants per powder weight (ppw) with 1 M HCl and NaOH solutions. The titrations were performed from the initial pH of the dispersions (approx. pH 5) up to pH 11 (leg 1) and then from pH 11 down to pH 3 (leg 2). The results of leg 2 are reported in this paper and used for analysis. The conductivity was 0.5–1.2 mS/cm for all systems during leg 2.

Thermogravimetric analysis (TGA) of adsorbed dispersant

Dispersant adsorption on Al_2O_3 was assessed by thermogravimetric analysis (TGA), (Mettler-Toledo, Switzerland TGA/DTA 851) of powders with and without adsorbed dispersants. Four weight percent of Al_2O_3 dispersions were equilibrated with different amounts of dispersant over a period of 12 h. The powders were centrifuged at 10,000 rpm, decanted, and the deposit was dried in an oven at 80 °C overnight. The TGA heating profile consisted of a 5 °C/min ramp and a 30 min soak at 100 °C to remove weakly adsorbed water followed by a 5 °C/min ramp to 700 °C, ensuring the organic part of the dispersant is totally removed. Results were normalized to the weight of samples after the soak at 100 °C. The weight loss is calculated from the interval 100–700 °C. This weight loss corresponds to the maximum weight loss in this system since the comb polymer interacts via its carboxylic groups with the hydroxyl groups on the powder surface in solution and during the soak at 100 °C, which leads to a reduced weight loss between 100 and 700 °C [4, 24]. The weight loss of the Al_2O_3 powder without dispersant in the 100–700 °C temperature range averaged 0.74 %. This value is subtracted from the weight loss of dispersant to obtain a value for the minimum adsorbed dispersant [4, 24] as it corresponds to a total removal of the hydroxyl groups. However, the interaction of the comb polymers with the particle's surface is expected to be dependent on the dispersant coverage, hence dosage (in wt% ppw) as well as charge density. The use of maximum and minimum values is limited since anomalously high maximum values (>100 %) or anomalously low (even negative) minimum values are obtained. In this work, we have used the empirical formula below to correct for the undetected weight loss due to comb polymer-Al_2O_3 interactions:

$$Corrected\,weight\text{-}loss = Minimum\,weight\text{-}loss + 0.74\cdot\left(1-CHU/7\right)^{2.9}\cdot\left(CCFN/2.975\right)^{2} \quad (1)$$

where CCFN is a comb polymer dependent charge/composition factor which is developed and discussed in the next Section and CHU=dosage (wt% ppw)·CCFN. At higher dispersant dosage (>2–3 %), the correction converges rapidly to the minimum weight loss values. At lower dispersant dosage, the correction leads to realistic values which are higher than the minimum values but never exceeding 100 % (or the maximum weight loss if <100 %). In addition, the corrected weight loss above, which accounts for the organic part of the dispersant, is corrected for the inorganic part by taking in account the known sodium content of the comb polymers which appears in Table 2 [4, 22, 24]. The corrected values are used for the determination of the adsorbed dispersant weight per unit area in mg/m^2 calculated by dividing by the surface area of the powder.

Results and discussion

Normalization charge/composition factors of a repeating unit (CCF and CCFN)

Figure 1 and Table 1 show the architecture and exact (yet statistical) composition of the comb polymers studied in this work. Due to the known molecular architecture, it is possible to calculate for each comb polymer a simple charge/composition factor (CCF)≡(number of charged groups in

Table 2 Development of CCF and CCFN charge density normalization factors for comb polymer dispersants

	B174	B176	B178	B179
Charged groups/total groups in one repeating unit $n_{RU}/(n+m)_{RU}$	2/3	6/7	2/3	6/7
Molecular weight of one repeating unit $MW_{RU}=(44\cdot p+15)\cdot m+(n+m)\cdot 85+ n\cdot 23$ (or $n\cdot 1$) (g/mol)	1328 (1284)	1760 (1628)	4804 (4760)	5236 (5104)
Na content (%)	3.42	8.10	0.924	2.59
$CCF\equiv n_{RU}/MW_{RU}$ (mol/g)	$1.51\cdot10^{-3}$ ($1.56\cdot10^{-3}$)	$3.41\cdot10^{-3}$ ($3.68\cdot10^{-3}$)	$4.16\cdot10^{-4}$ ($4.20\cdot10^{-4}$)	$1.15\cdot10^{-3}$ ($1.18\cdot10^{-3}$)
$CCFN_i\equiv CCF_i/CCF_{179}$	1.314 (1.325)	2.975 (3.135)	0.363 (0.357)	1 (1)

Number in brackets indicate composition without Na counter ion

one repeating unit)/(molecular weight of one repeating unit) based solely on the chemical formula of the dispersant. The usefulness of such charge density factors will become apparent in the next sections. Somewhat similar approach to develop charge/composition factors was developed in reference [20], where the charge units (acid groups) were determined by titrations. However, their study which was conducted with comb polymers having side-chain lengths in the 475–2,000 g/mol range resulted in factors in the range 2.4–4.4, a range which was concluded by the authors to be too small to have significant effects on the conformation of comb polymers in solution or other properties [20]. The CCF values for the four dispersants in the present study are shown in Table 2 as well as the dimensionless CCF values $CCFN_i = CCF_i/CCF_{179}$ which are the CCF values in (charge units·mol)/g normalized to the CCF value of B179 and therefore more convenient for use. Note that two values of CCF are given in Table 2, those excluding and those including the counter ion Na. Values excluding Na appear in brackets. The CCFN factors including Na are used in this paper. The use of Na free values introduces only small deviations. A practical consideration for using the CCF values including Na is that it is directly related to the dosage of dispersant.

As can be seen in Table 2, the CCF and CCFN values are dependent on both charge frequency and molecular weight in one repeating unit of the comb polymer. In other words, the CCFN is a measure of the relative charge density per unit weight of the polymers. In this work, the CCFN factors span about an order of magnitude from 0.363 for the low charge/long chain (B178) to 2.975 for the high charge/short chain comb polymer (B176).

Conductivity of the dispersants in DI water

The conductivity of the comb polymers in DI water is shown in Fig. 2a as a function of their concentration in solution. The conductivity shows a linear dependence on comb polymer concentration in all cases (R^2>0.999) with linear regression coefficients between 23–366 (μS cm^2)/g, more than an order of magnitude. A gradual decrease in conductivity is observed with decrease in charge density from the high charge/short chain to the low charge/long chain polymers. Figure 2b shows the conductivity of the polymers as a function of their concentration linearly normalized by the CCFN values computed in Table 2.

Except B178, all three polymers fall essentially on the same curve, with linear regression coefficients of 129.5±5 (μS cm^2)/g indicating a certain universality of the CCFN values for the conductivity in solution. The low charge/long chain B178 shows a linear regression coefficient of only 64, roughly half than that of the other dispersants, suggesting the conductivity in this case is also significantly dependent on conformation effects of this low charge/long chain comb polymer [20]. Nevertheless, also for B178 the values after normalization are significantly closer. As suggested by one of the reviewers, the conductivity of the dispersant solutions can be also used (after calibration) to assess the concentration of the dispersants in solutions. For example, conductivity measurements of the supernatant solutions can be used for determination of adsorption data.

Zeta potential and dispersant adsorption during dispersant titrations

Figure 3a shows the evolution of zeta potential and pH of the Al_2O_3 dispersions during titration with the four dispersants. The zeta potential of the dispersions without dispersants of about +118 mV at a pH value of 4.2–4.4 is decreased with the addition of the anionic comb polymer dispersants. The initial rate of decrease in zeta potential is relative to the charge density of the dispersants or the trend of conductivity in solution shown previously in Fig. 2.

The corresponding pH change shown in Fig. 3b shows an increase to a maximum value which occurs just after the end of the steep change in the zeta-potential curve. At a pH value of 4.97–5.00, a maximum in the pH curve is observed for all dispersants. Such behavior has been seen in commercial comb

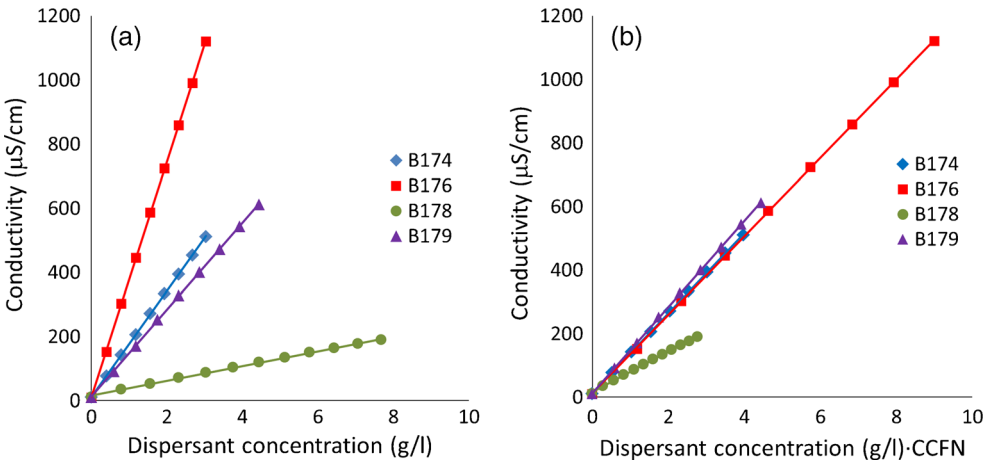

Fig. 2 **a** Conductivity of the comb polymers in DI water. **b** Conductivity of the polymers as a function of their concentration linearly normalized by the CCFN values computed in Table 2

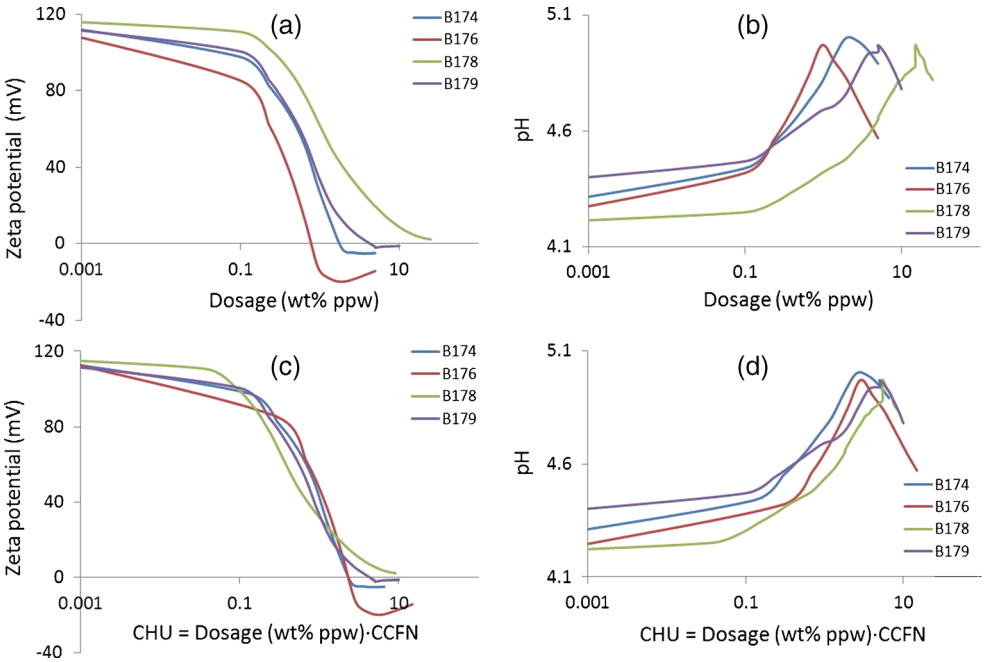

Fig. 3 Evolution of zeta potential and pH of the Al_2O_3 dispersions during titration with the four dispersants. **a** Zeta and **b** pH as a function of dispersant dosage. **c** Zeta and **d** pH as a function of CHU (dispersant dosage normalized by CCFN)

polymer systems and can be interpreted on the basis of ligand exchange or charge regulation mechanisms [24, 29, 30].

Figure 3c shows the zeta potential values shown in Fig. 3a where a normalized dosage, CHU≡dosage (wt% ppw)·CCFN is plotted on the abscissa. The CHU represents normalized charge units (charge units/molecular weight)$_{RU}$·dosage= charge units number of units=count of charge units (here, normalized relative to B179). As in the case of the ionic conductivity, the use of CCFN normalization leads to significant overlap of the zeta potential and pH curves in Figs. 3c, d, respectively. B178 shows also here somewhat larger deviations than the other three dispersants, but much better similarity after normalization is obtained. Despite the apparent overlap of the curves in Figs. 3c, d, the zeta potential and pH curves show several features which cannot be normalized by the linear transformation using the CCFN values. Nevertheless, we find that the CCFN can be correlated directly with features extracted from Fig. 3a, b. Figure 4a shows curve fitting of the zeta potential data of the comb polymers during dispersant titration from Fig. 3. Here, only positive zeta potential values are presented. All comb polymers exhibit an exponential decay with dispersant dosage. Table 3 shows the summary of the curve fitting parameters for the exponential functions which are shown as the dashed black lines in Fig. 4a.

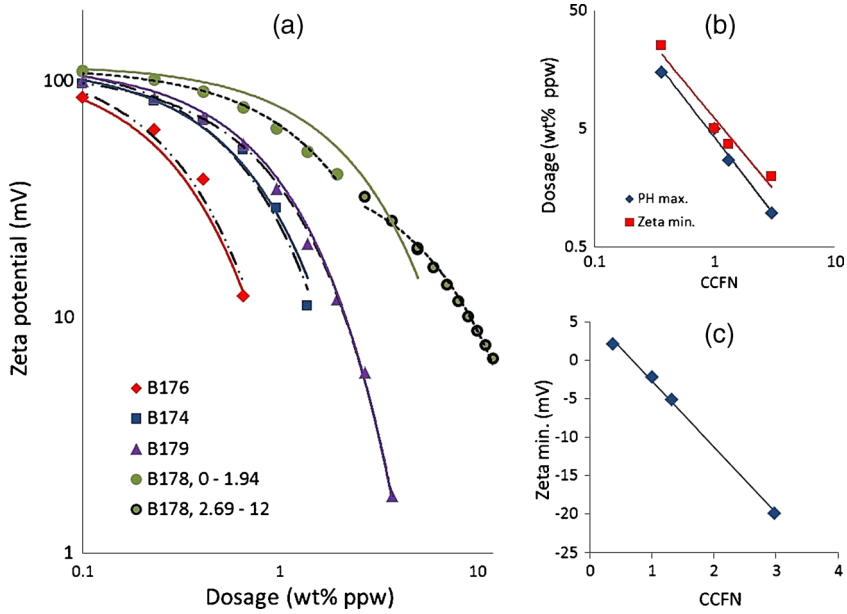

Fig. 4 Curve fitting of the zeta potential data of the comb polymers during dispersant titration from Fig. 3 **a** Zeta potential as a function of dosage. **b** dosage at pH_{max} and $Zeta_{min}$ as a function of CCFN. **c** $Zeta_{min}$ as a function of CCFN

Table 3 Curve fitting parameters for $\zeta = M \cdot \exp(-N \cdot \text{dosage})$ in Fig. 4

Dispersant	CCFN	Dosage range (wt% ppw)	Zeta potential range (mV)	M	N	R^2
B176	2.975	0–0.65	118.0–12.7	126.3	3.376	0.978
B174	1.314	0–1.94	118.4–11.9	124.9	1.663	0.9801
B179	1	0–3.68	116.3–1.76	110.0	1.125	0.998
B178, 0–1.94	0.363	0–1.94	117.9–40.40	115	0.57	0.9912
B178, 2.69–12	0.363	2.69–12	32.43–6.7	46	0.166	0.991

Also here, as in the case of the conductivity of the comb polymers in solution (Fig. 2), B178 is singled out.

While the three comb polymers B176, B174, and B179 show excellent agreement to a single exponential function, B178 shows a limited range of correlation and requires two exponential functions to describe the zeta potential in the dosage range of 0–12 wt% ppw. Both functions are summarized in Table 3 and appear as the dotted black lines in Fig. 4a.

The solid lines in Fig. 4a plots Eq. (2)=F (dosage, CCFN) where M is set to 118 mV and $N = 1.15 \cdot \text{CCFN}$. The fit of Eq. (2) for B176, B174, and B179 to the experimental zeta potential values as well and the original exponential fits (dashed lines) is excellent. The fit for B178 is relatively good and appears as a good compromise, considering that $1.15 \cdot 0.363 = 0.417$ for this dispersant falls between the exponents of 0.57 and 1.66 found in Table 3 for the short range and long range results, respectively. The significance of the results above is twofold: (1) they indicate that the dependence of zeta potential of colloids on dispersant dosage can be expressed by exponential functions and (2) the exponents are directly related to the CCF factors in the case of comb polymers. Note that the apparent similarity between the absolute values of the CCFN and the exponents in Table 3 are coincidental, since the normalization of the CCFN using CCF_{179} was chosen at random.

$$\zeta = \text{M} \cdot \exp(-N \cdot \text{dosage}); \text{M} = 118\text{mV}, \text{N} = 1.15 \cdot \text{CCFN} \quad (2)$$

In addition, we find that the dosage associated with the minimum in zeta potential (ζ_{min}) and the maximum in the pH (pH_{max}) seen in the curves of Figs. 3a, b, respectively, show clear dependency on CCFN (Fig. 4b). These, which are related to similar charge neutralization processes, show a very similar power law dependency on CCFN, namely dosage (pH_{max}) $\propto \text{CCFN}^{-1.32}$ and dosage (ζ_{min}) $\propto \text{CCFN}^{-1.23}$. It is interesting to note that pH_{max} always precede ζ_{min}. In fact, the dosage (pH_{max}) appears to correspond to the dosage value just after the steepest change in zeta potential seen in Fig. 3a. ζ_{min}, the minimum Zeta potential itself is also found to be dependent on the CCFN (Fig. 4c) and shows a linear regression coefficient of −8.55 mV indicating significant dependence on CCFN and allows direct determination of the minimum zeta potential for this system based on the CCF values alone. Ran et al. which have compared dispersant titrations of comb polymers of similar frequency but different side-chain lengths have observed a similar trend in zeta potential [26]. The dependence of ζ in general and ζ_{min} in particular is related to both increased surface charge neutralization effects of high CCFN dispersants and a shift in the plane of zeta potential due to adsorbed layer thickness which is related to the length of the side-chains. Both effects are discussed latter in the manuscript in conjunction with dispersant adsorption and potentiometric titrations.

The explicit relationships in Fig. 4 can be used for almost full reconstruction of Fig. 3a and thus can serve as design tools for new dispersants based on functions of CCFN alone.

Figure 5a shows the adsorbed dispersant weight per surface area of the Al_2O_3 powder in mg/m^2 and the adsorption efficiency η defined as (weight adsorbed)/(dosage) as a function of dispersant dosage. As expected, the adsorption efficiency

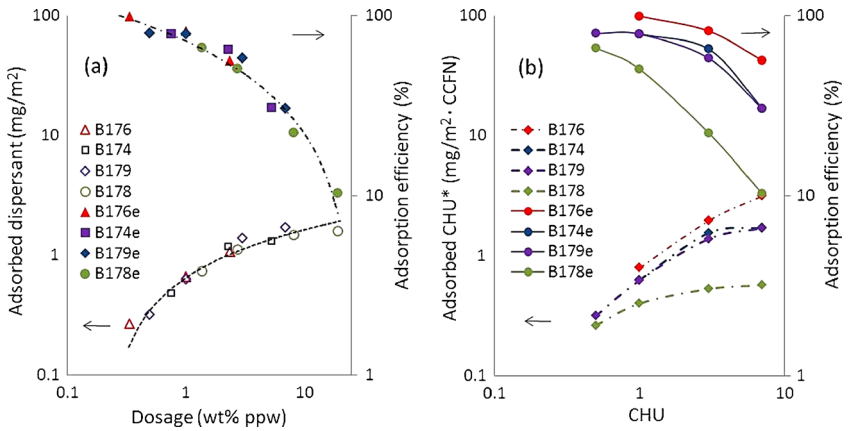

Fig. 5 **a** Adsorbed dispersant weight per surface area of the Al_2O_3 powder in mg/m^2. **b** Efficiency and adsorbed dispersant as a function of CFU

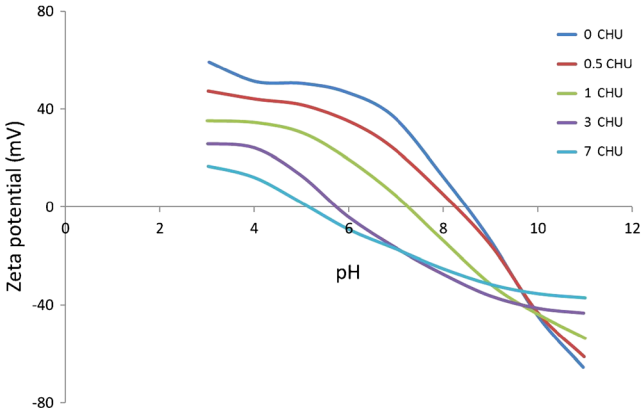

Fig. 6 Potentiometric titration of Al_2O_3 dispersions containing B174 dispersant with varying CHU

decreases and the adsorbed dispersant weight increases with dosage. Irrespective of their molecular architecture, all dispersants show very similar behavior as a function of dosage and conform, within the dosage studied, to the logarithmic curves shown by the solid lines in Fig. 5a. The adsorbed dispersant per powder unit area can be expressed by adsorbed dispersant (mg/m^2)=−21.79·ln (dosage)+72.2 and the efficiency by η= 0.43·ln (dosage)+0.65.

B179 does show in Fig. 5a slightly higher values than the other dispersants probably due to the fact that it has both high charge and long chains. Our results differ somewhat from other works which have studied adsorption of different comb polymers (e.g., with different chain lengths) [25, 26]. This is likely due to the fact that we focused our work on the CHU values, and not all dispersants have reached the plateau of adsorption. Nonetheless, Fig. 5b shows the efficiency and adsorbed dispersant as a function of CFU, where the adsorbed dispersant is expressed by normalized charge units CHU* (defined slightly different for this case as the adsorbed dispersant $mg/m^2 \cdot CCFN$). In this representation, a clear trend is established, where the higher CCFN comb polymers exhibit higher efficiencies and higher charge adsorption values. This result is consistent with the trends seen in the zeta potential results in Fig. 3 and more clearly in Fig. 4, where the rate of change in zeta potential (Fig. 4a) and its absolute magnitude of the minimum values (Fig. 4c) are increased with the CCFN.

Zeta potential during potentiometric titrations

Potentiometric titrations were conducted with dispersions containing different dispersant concentrations. The results are presented as a function of CHU which normalizes charge effects. Before comparing the different dispersants, it is worthwhile to observe the general trend for one dispersant. Figure 6 shows an example of a set of potentiometric titrations of dispersions containing B174 dispersant with CHU values ranging from 0–7 CHU. Figure 6 indicates an overall decrease in zeta potential magnitude with the CHU and a gradual shift of the isoelectric point to the acidic range, as can be expected from the increase in dispersant and charge adsorption seen in Fig. 5a, b, respectively.

Figure 7 presents the potentiometric titrations of all comb polyelectrolytes at four different CHU values. The decrease in zeta potential and the shift of the isoelectric point for all dispersants with the CHU are apparent. In addition, this representation which largely normalizes charge effects highlights the chain-length effects of the comb polymers. Here, the long chain B179 and B178 pair are clearly distinguished from the short chain pair in all the pH range studied, especially from

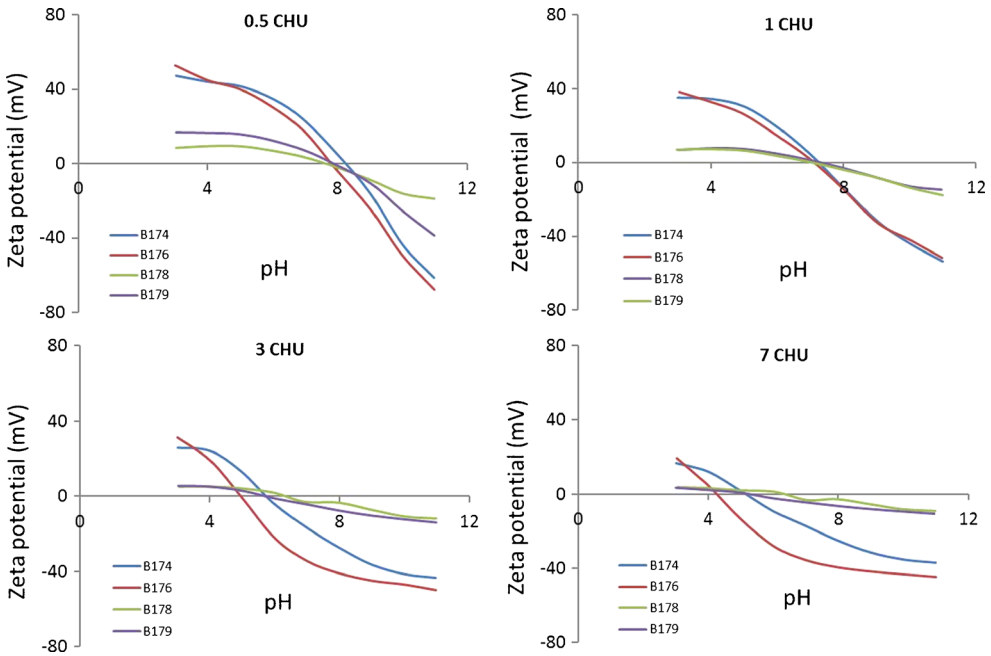

Fig. 7 Comparison of potentiometric titration of Al_2O_3 dispersions with different comb polymer dispersants at CHU values of 0.5, 1, 3 and 7

CHU values >1. B174 and B176 do show deviations from each other, especially apparent at pH>IEP, but at the same time are well distinguished from the long chain pair. In other words, no continuous trend is observed based on charge consideration, as would be expected from Fig. 5b. In particular, B179 and B174 which showed in the previous sections very similar zeta potential (Figs. 3 and 4) and adsorbed charge values (Fig. 5b) are clearly very different in their zeta potential response to pH at fixed CHU. The reason for the pairing of the dispersants according to their side-chain length observed in Fig. 7 is likely to be a shift in the shear plane due to an adsorbed dispersant thickness observed for non-ionic polymers [31], an effect which may be highlighted in potentiometric titration due to increased ionic strength leading to compression of the double layer. This effect is equally important for comb polymers having non-ionic side-chains [26, 32]. A simplified illustration of this effect can be understood by superposition of the electrical double layer with a zeta potential plane located at a distance d from the surface of the particle and an adsorbed comb polymer dispersant having an effective side-chain length l. If $l<d$, no shift of the zeta potential plane occurs and the measured zeta potential is not affected. However, if $l>d$, the side-chains extend beyond the original location of the zeta potential plane. Since the side-chains are anchored to the particle surface and move with the particle, the location of their tips now determines the shear plane. This new plane which is farther away from the particle surface compared to the original plane causes a shift of the zeta potential to lower values. According to the results shown in Fig. 7, it appears that this effect strongly influences the long side-chain comb polymers B178 and B179 having a side-chain composed of 102 EO units and the short side-chain B176 and B174 having 23 EO units (Table 1) to a much lesser degree. We use interpolation of the results provided by Roosjen et al. [33] which provide a realistic approximation of brush lengths for PEO brushes with up to 222 EO units and obtain the values of about 14.6 and 4.4 nm for the long chain (102 EO units) and short chain (23 EO units) dispersants, respectively. For reference, the conductivity values during potentiometric titrations were between 0.5–1.2 mS/cm indicating Debye length $1/\kappa<5$ nm in agreement with the behavior of the long chain dispersants seen in Fig. 7.

Table 4 Curve fitting parameters for IEP=A (dosage)^B in Fig. 8a

Dispersant	CCFN	A	B	R^2
B176	2.975	5.1763	0.244	0.9800
B174	1.314	6.865	0.184	0.9931
B179	1	7.0356	0.167	0.9918
B178	0.363	7.8041	0.072	0.9509

As discussed in the previous Section, Ran et al., who compared the zeta potential of comb polymers with 4–45 EO units, have observed a systematic decrease of the zeta potential during dispersant titrations with the increase in side-chain length [26], in agreement with our results in Figs. 3 and 4c. They have interpreted the results based entirely on a continuous shift of the shear plane. However, as stated above, such shift is not likely to be observed for comb polymers having short side-chains with $l<d$, especially at low ionic strength. Our results in Fig. 3 and 4 indicate that contributions of both charge and side-chain length play a role in determining both CCFN values and zeta potential during dispersant titrations.

One point which is difficult to detect in Fig. 7, especially for the long chain comb polymers, are the values for the

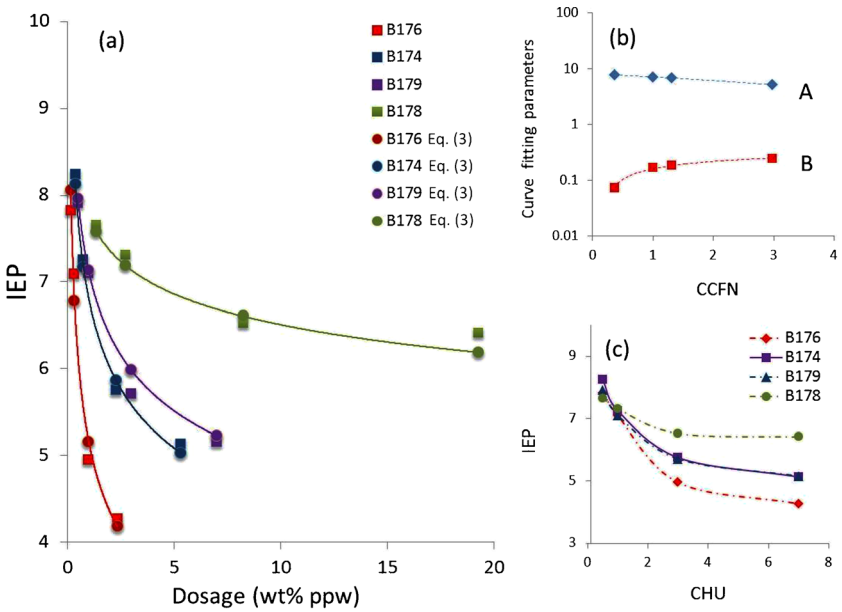

Fig. 8 **a** IEP of Al_2O_3 dispersions with different comb polymer dispersants as a function of dosage. **b** curve fitting for the parameters A and B in Eq (3). **c** IEP as a function of CHU

isoelectric point (IEP). Figure 8a shows a summary of the IEP of the dispersions as a function of dispersant dosage (square symbols). Plotted in this way, it is apparent that the higher the CCFN of the dispersants the larger the rate of decrease in IEP per wt% ppw of dispersant. The IEP, at a first approximation, is independent on the shift of shear plane seen in Fig. 7. Therefore, the IEP appears as a very sensitive tool for the effect of the CCFN, in very good agreement with the trend seen in Fig. 4c especially (in a "mirror symmetry") to the CHU* adsorption values found in Fig. 5b.

All curves can be fitted with a power law function. The summary of the results are given in Table 4. In addition, the constant A and the power law exponent B can be directly expressed as functions of CCFN as postulated in Eq (3). The fit of these functions to the values obtained in Table 4 is seen in Fig. 8b. We find $A=-0.9924\cdot CCFN+8.1225$ and $B=0.0819\cdot \ln(CCFN)+0.1596$ with excellent agreement ($R^2>0.99$). Eq. (3), now expressed with the equations above as: IEP=F (dosage, CCFN) is plotted in Fig. 8a for all comb polymers using the solid lines as well as round symbols. The excellent agreement to the experimental points is evident. Also here, as in the case of the zeta potential in Fig. 4, the results indicate that (1) the IEP of colloids as a function of dispersant dosage can be expressed by power law functions and (2) the power law exponents are directly related to the CCF factors in the case of comb polymers.

Figure 8c which re-plots the data in Fig. 8a as a function of CHU reveals an intersection point at CHU=1, where all dispersants lead to a similar isoelectric point (7.09–7.31). At CHU>1, the trend is similar to that seen in Fig. 8a where higher CCFN dispersants lead to lower IEP for a given CHU. At CHU<1, no clear trend can be observed but the values appear to diverge. This phenomenon point is not completely clear as it relies on only one experimental point and requires more elucidation. Nevertheless, the existence of the intersection point at CHU=1 may relate to the trend observed in Fig. 7 (1 CHU) where the pairs of similar chain lengths show very similar same zeta potentials at all pH values measured.

$$\mathrm{IEP} = \mathrm{A}(dosage)^{B};\ \mathrm{A} = \mathrm{f}_1(CCFN),\ \mathrm{B} = \mathrm{f}_2(CCFN) \qquad (3)$$

Conclusions

In this work, we studied the effect of comb polymer molecular architectures on the properties of Al_2O_3 colloidal dispersions. Four PMAA-PEO (sodium salt) comb polymers with varying charge frequency and chain length were tested.

A central theme in this manuscript is the development of a simple charge/composition factor (CCF) calculated based only on the known molecular architecture of the comb polymers. The normalized factors (CCFN) calculated for the comb polymers studied span about an order of magnitude and range from 2.975 for the short chain/high charge comb polymer to 0.363 for the long chain/low charge comb polymer. The CCFN are used for the first time in explicit functions to correlate and explain the data as well as normalization factors to obtain a quantity representing charge units (CHU) defined as CHU≡dosage·CCFN.

We demonstrate here for the first time that the conductivity of the dispersants scales directly with the CHU. The zeta potential during dispersant titration and the isoelectric point (IEP) of the dispersions as a function of dispersant dosage can be fitted precisely by exponential and power law functions, respectively, where the coefficients are functions of CCFN as a single variable. Representation of the adsorption in charge units by CCFN normalization ($mg/m^2\cdot CCFN$) and plotting it and the adsorption efficiency as a function of CHU show clear trends of increased efficiency and charge adsorbed with the CCFN, consistent with the behavior found in the IEP results and zeta potential during dispersant titration.

Our results provide a clear and quantitative link between dispersant molecular architecture and zeta potential, IEP of dispersions as well as dispersant conductivity in solutions and thus provide a unique tool for the design of new and improved dispersants.

In addition, we observe a linear decrease of the minimum zeta potential with the CCF which is dependent on both chain length and charge frequency. Potentiometric titrations as a function of CHU indicate that the shift of the shear plane is only significant for the long side-chain comb polymers (consisting of 102 EO units).

Acknowledgments The authors wish to thank Dr. Joachim Pakusch and Dr. Stefan Becker (BASF AG, Ludwigshafen, Germany) and Frank Winnefeld (Empa, Dübndorf, Switzerland) for the comb polymer dispersants.

References

1. Studart AR, Amstad E, Antoni M, Gauckler LJ (2006) J Am Ceram Soc 89:2418–2425
2. Lewis JA (2000) J Am Ceram Soc 83:2341–2359
3. de Hazan Y (2012) J Am Ceram Soc 95:177–187
4. de Hazan Y, Knies F, Burnat D, Graule T, Yamada-Pittini Y, Aneziris C, Kraak M (2012) J Colloid Interface Sci 365:163–17
5. Flatt RJ, Houst YF (2001) Cem Concr Res 31:1169–1176
6. Kirby GH, Lewis JA (2004) J Am Ceram Soc 87:1643–1652
7. Winnefeld F, Becker S, Pakusch J, Götz T (2007) Cem Concr Compos 29:251–262
8. Felekoglu B, Sarıkahy H (2008) Constr Build Mater 22:1972–1980
9. Zingg A, Winnefeld F, Holzer L, Pakusch J, Becker S, Gauckler L (2008) J Colloid Interface Sci 323:301–312
10. Ran Q, Somasundaran P, Miao C, Liu J, Wuc S, Shen J (2009) J Colloid Interface Sci 336:624–633
11. Plank J, Sachsenhauser B (2006) J Adv Concr Technol 4:233–239
12. Houst YF, Bowen P, Perche F, Kauppi A, Borget P, Laurent G, Le Meins JF, Lafuma F, Flatt RJ, Schober I, Banfill PFG, Swift DS, Myrvold BO, Petersen BG, Reknes K (2008) Cem Concr Res 38:1197–1209
13. Plank J, Pöllmann K, Zouaoui N, Andres PR, Schaefer C (2008) Cem Concr Res 38:1210–1216

14. Ferrari L, Kaufmann J, Winnefeld F (2010) J Plank. J Colloid Interface Sci 347:15–24
15. D. Marchon, U. Sulser,A. Eberhardt, R.J. Flatt, Soft Matter, DOI: 10.1039/c3sm51030a.
16. Alonso MM, Palacios M, Puertas F (2013) Cem Concr Compos 35:151–162
17. Laarz E, Bergström L (2000) J Eur Ceram Soc 20:431–440
18. Laarz E, Kauppi A, Andersson KM, Kjeldsen AM, Bergström L (2006) J Am Ceram Soc 89:1847–1852
19. Kjeldsen AM, Flatt RJ, Bergström L (2006) Cem Concr Res 36:1231–1239
20. Yoshikawa J, Lewis JA, Chun BW (2009) J Am Ceram Soc 92:S42–S49
21. Bouhamed H, Boufi S, Magnin A (2009) J Colloid Interface Sci 333:209–220
22. de Hazan Y, Heinecke J, Weber A, Graule T (2009) J Colloid Interface Sci 337:66–74
23. de Hazan Y, Märkl V, Heinecke J, Aneziris C, Graule T (2011) J Eur Ceram Soc 31:2601–2611
24. de Hazan Y, Reuter T, Werner D, Clasen R, Graule T (2008) J Colloid Interface Sci 323:293–300
25. Bouhamed H, Boufi S, Magnin A (2007) J Colloid Interface Sci 312:279–291
26. Ran Q, Qiao M, Liu J, Miao C (2012) Colloid Polym Sci 290:435–443
27. Gay C, Raphael E (2001) Adv Colloid Interf Sci 94:229–236
28. Flatt RJ, Schober I, Raphael E, Plassard C, Lesniewska E (2009) Langmuir 25:845–855
29. Wolterink JK, Koopal LK, Stuart MAC, Van Riemsdijk WH (2006) Colloids Surf A Physicochem Eng Asp 291:13–23
30. Sakar-Deliormanlı A, Celik E, Polat M (2008) ColloidS Surf A Physicochem Eng Asp 316:202–209
31. Carasso ML, Rowlands WN, O'Brien RW (1997) J Colloid Interface Sci 193:200–214
32. Plank J, Vlad D, Brandl A, Chatziagorastou P (2005) Cem Int 3:100–110
33. Roosjen A, van der Mei HC, Busscher HJ, Norde W (2004) Langmuir 20:10949–10955